Enhanced Concentration Fluctuations in Polymer Solutions under Shear Flow

X.-L. Wu
Department of Physics, University of Pittsburgh, Pittsburgh, Pennsylvania 15260

D. J. Pine and P. K. Dixon
Exxon Research and Engineering Co., Annandale, New Jersey 08801
(Received 10 January 1991)

We report an elastic-light-scattering experiment for a semidilute polymer solution under a uniform laminar shear flow. The concentration fluctuations are greatly enhanced by shear flow and their structure is highly anisotropic in both the weak ($\dot{\gamma}\tau_d \ll 1$) and strong ($\dot{\gamma}\tau_d \gg 1$) shear regimes, where $\dot{\gamma}$ is the shear rate and τ_d is the longest relaxation time of the system. The anisotropy is qualitatively different from binary liquid mixtures under a shear flow as a result of the strong coupling between the concentration fluctuations and the hydrodynamic flow.

PACS numbers: 82.70.Kj, 66.90.+r, 82.70.Dd

It is well known that entangled polymer solutions near phase separation undergo significant changes when subjected to shear flow. The most notable effect is a dramatic increase in turbidity which, since its discovery nearly twenty years ago, has been interpreted as evidence of a shear-induced phase transition.[1,2] There are well-documented cases of shear-induced changes in the phase behavior of other systems: simple binary liquid mixtures,[3,4] binary polymer melts,[5] and binary polymer solutions.[6] However, in these systems, shear flow *suppresses* concentration fluctuations, turbidity, and phase separation. Furthermore, the shear-induced effects are much smaller than in polymer solutions. In binary liquid mixtures, for example, the turbidity is reduced by shear only within $\sim 0.1\,^{\circ}\mathrm{C}$ of the critical temperature and only for shear rates exceeding $\dot{\gamma} \sim 1000\ \mathrm{s}^{-1}$.[3] By contrast, in polymer solutions, the turbidity can be enhanced for temperatures of more than $50\,^{\circ}\mathrm{C}$ above the phase-separation temperature at shear rates of less than $10\ \mathrm{s}^{-1}$.

Recently, the existence of a shear-induced change of the phase transition in semidilute polymer solutions has been called into question by a number of investigators.[7-9] Part of the controversy centers around questions of how to treat the thermodynamics of these nonequilibrium systems. An even more pressing issue is the question of the mechanism for the shear-induced enhancement of the concentration fluctuations which leads to the increased turbidity. Several conflicting mechanisms have been proposed.[2,7,8] However, progress on these problems has been hampered by a lack of detailed experimental information about the structure of sheared polymer solutions.

In this paper, we present light-scattering measurements of the nonequilibrium steady-state structure factor $S(\mathbf{q},\dot{\gamma})$. Our results support a mechanism proposed by Helfand and Fredrickson[7] in which concentration fluctuations are enhanced by a coupling between the polymer concentration and shear flow through the concentration-dependent viscosity and normal stress coefficients.[7,9-11] In contrast to previous experiments, we do not find evidence of a shear-induced shift in the phase boundary at low rates of shear. At higher rates of shear, a shear-induced transition remains an intriguing possibility.

Our samples consisted of a volume fraction $\phi = 0.04$ of polystyrene (PS) dissolved in dioctylphthalate (DOP). The polystyrene has a molecular weight of $\bar{M}_w = 1.8 \times 10^6$ and a polydispersity of $\bar{M}_w/\bar{M}_n = 1.03$. This gives a radius of gyration $R_g \simeq 250$ Å, and an overlap concentration $\phi^* \simeq 0.008$. Thus, the solution is well into the semidilute regime. To characterize the rheological properties of the sample, we measured the dynamic viscosity $\eta(\omega)$ over angular frequencies $0.01\ \mathrm{s}^{-1} < \omega < 100\ \mathrm{s}^{-1}$. The data define a characteristic rheological time τ_d such that for $\omega\tau_d \ll 1$, $\eta = \eta_0$ is a constant, and for $\omega\tau_d \gg 1$, $\eta \sim \omega^{-2/3}$. For $T = 15\,^{\circ}\mathrm{C}$, $\tau_d = 0.57$ s and $\eta_0 = 270$ P. The viscosity of pure DOP at $15\,^{\circ}\mathrm{C}$ is ~ 1 P.

Our experiment was performed in a transparent Couette cell with the inner cylinder rotating. The scattering geometry is shown in Fig. 1. The index of refraction of DOP at room temperature is 1.48, which closely matches the Pyrex glass from which the cell was made. In addition, the Couette cell was immersed in an index-matching fluid to minimize beam deflection and stray light. The index-matching fluid also served as a thermal bath whose temperature was controlled to $\pm 0.2\,^{\circ}\mathrm{C}$. A weakly focused horizontal He-Ne laser beam illuminated a small scattering volume in the gap (~ 1 mm) formed by the two cylinders. The intensity of light scattered from the solution through different angles ($0^{\circ} < \theta < 180^{\circ}$) was measured using a photomultiplier tube. The scattering wave vector, $\mathbf{q} = \mathbf{k}_o - \mathbf{k}_i$, was confined to the horizontal plane, defined by $\mathbf{v}$ and ∇v, as shown in Fig. 1. In a uniform shear flow the concentration fluctuations become spatially anisotropic so that the

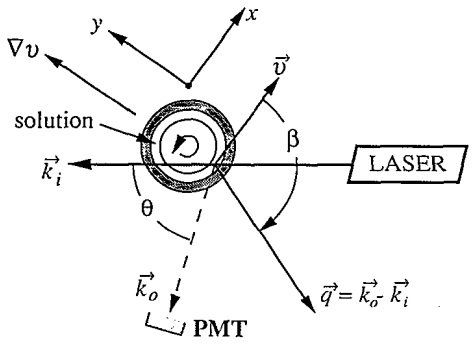

FIG. 1. Couette-cell scattering geometry. Coordinates are defined with $\mathbf{x}\|\mathbf{v}$ and $\mathbf{y}\|\nabla v$; $\mathbf{k}_i$, $\mathbf{k}_o$, and $\mathbf{q}$ are the incident, output, and scattering wave vectors, respectively. The magnitude of $\mathbf{q}$ is set by the scattering angle θ, with $q=2k_i\sin(\theta/2)$; the direction of $\mathbf{q}$ is varied by rotating the cell about the scattering volume and varying β. For the geometry depicted, $\beta=-112°$.

scattering intensity depends on both the magnitude and direction of $\mathbf{q}$ relative to the flow direction. We define the direction of $\mathbf{q}$ relative to the flow by the angle β between $\mathbf{v}$ and $\mathbf{q}$ (see Fig. 1). In order to independently vary θ and β, the cell was mounted on a rotation stage with the axis of the stage aligned vertically with the scattering volume.

In this experiment we measured the relative scattering intensity, $I(\mathbf{q},\dot\gamma)/I_0(\mathbf{q},0)$, for twenty shear rates between 0 and 10 s^{-1}. Here $I(\mathbf{q},\dot\gamma)$ is the scattering intensity at a constant shear rate $\dot\gamma$ and $I_0(\mathbf{q},0)$ is the scattering intensity in the quiescent state. This relative measurement is useful because $I(\mathbf{q},\dot\gamma)/I_0(\mathbf{q},0)$ is independent of the size of the scattering volume and facilitates quantitative comparisons of scattering intensity at different angles. We convert this relative intensity measurement to the nonequilibrium structure factor $S(\mathbf{q},\dot\gamma)$ by multiplying $I(\mathbf{q},\dot\gamma)/I_0(\mathbf{q},0)$ by $S(\mathbf{q},0)$, the equilibrium structure factor. We measured $S(\mathbf{q},0)$ as a function of wave vector $\mathbf{q}$ and temperature T and found that it follows the usual Ornstein-Zernike behavior:

$$S(\mathbf{q},0)=\chi/[1+(q\xi)^2], \tag{1}$$

where $\chi=\chi_0(T/T^*-1)^{-1}$, $\xi=\xi_0(T/T^*-1)^{-1/2}$, and $\xi_0=24$ Å. The critical exponents have the usual mean-field values. The apparent transition temperature T^*, found by fitting the equilibrium scattering data by Eq. (1), was 10.1 °C and agrees well with visual observations. At $T=15°$, $S(\mathbf{q},0)$ is essentially constant over the range of q measured; thus, $S(\mathbf{q},\dot\gamma)\simeq I(\mathbf{q},\dot\gamma)/I_0(\mathbf{q},0)$.

In Fig. 2 we show contour plots of $S(\mathbf{q},\dot\gamma)$ in the $\mathbf{v}$-∇v or x-y plane at shear rates of $\dot\gamma=0.4$, 1.2, and 10 s^{-1}. Here we see a gradual evolution of the scattering patterns as the shear rate increases. In the weak shear region, where $\dot\gamma\tau_d<1$, $S(\mathbf{q},\dot\gamma)$ is anisotropic with the scattering enhanced in the first and third quadrants and reduced in the second and the fourth quadrants. At the lowest shear rate we measure, $\dot\gamma=0.2$ s^{-1}, the intensity maxima align at $\sim 40°$ with respect to the flow direction $\mathbf{v}(q_x)$. This is in marked contrast to the usual shear-flow-induced affine distortion of structure which orients the intensity maxima along $\beta\simeq 135°$. This has been observed in phase-separating binary liquid mixtures,[12] in strongly interacting colloidal suspensions,[13] and in simulations of simple fluids.[14] The observed distortion along $\beta\simeq 40°$ is unique to semidilute polymer solutions and is perhaps the most novel feature of our light-scattering measurements. In addition to the angular distortion of the structure factor, a new length scale develops under shear flow as indicated by the peak at $q_x\approx q_y\approx 10$ μm^{-1}.

As the shear rate increases toward the strong shear regime, $\gamma\tau_d\gg 1$, there is an increase in the scattering at *all* $\mathbf{q}$ and the scattering pattern as a whole rotates clockwise. The peak in $S(\mathbf{q},\dot\gamma)$ also becomes sharper and moves to lower q. At $\dot\gamma=1.2$ s^{-1}, $S(\mathbf{q},\dot\gamma)$ is nearly aligned with the flow direction and the scattering intensity at the peak position is about 5 times that of the quiescent state [see

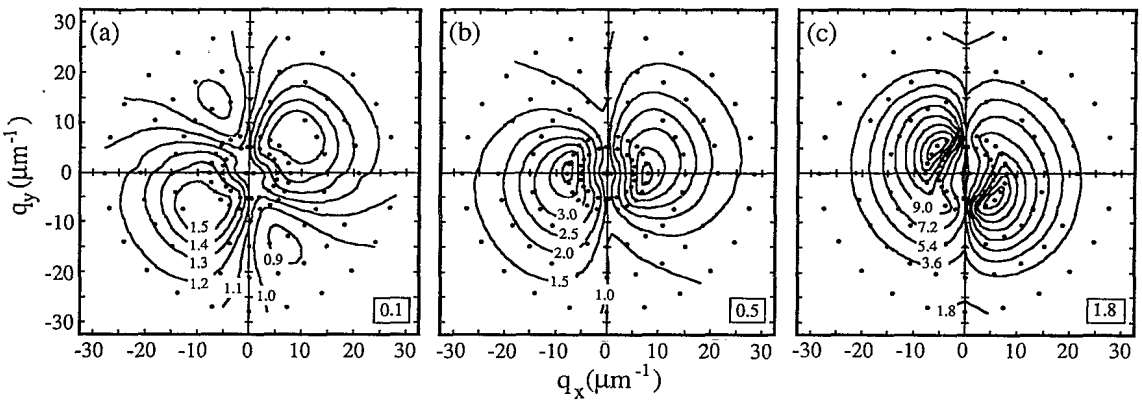

FIG. 2. Nonequilibrium steady-state structure factor $S(\mathbf{q},\dot\gamma)$: (a) $\dot\gamma=0.4$ s^{-1}, (b) $\dot\gamma=1.2$ s^{-1}, (c) $\dot\gamma=10$ s^{-1}. Solid circles indicate light-scattering measurements. Numbers in lower right indicate contour increments.

Fig. 2(b)]. Increasing the shear rate causes the scattering pattern to rotate further and the scattering intensity to grow. At $\dot{\gamma}=10\ s^{-1}$, the scattering maxima move beyond the flow direction and into the second and fourth quadrants. Note that the peaks remain at finite $\mathbf{q}$ and that their scattering intensity is nearly 20 times greater than the scattering intensity in the quiescent state. The increase in the scattering intensity over the quiescent state is least along the q_y axis. Scattering measurements were also performed at 11 and 25 °C. The results are similar to those shown in Fig. 2 except the magnitude of the scattering and the degree of rotation of $S(\mathbf{q},\dot{\gamma})$ is increased as the temperature is lowered.[15]

The dependence of the scattering on shear rate is shown in Fig. 3 for several cuts in the q_x-q_y plane. For $\beta=30°$, which is in the first quadrant of the q_x-q_y plane, the intensity increases monotonically with increasing shear rate. By contrast, for $\beta=120°$, which is in the second quadrant, the intensity initially decreases at low shear rates, goes through a minimum at $\dot{\gamma}_{\min}\simeq 0.6\ s^{-1}$, and then increases with increasing shear rate. For $\beta=90°$, the intensity is unaffected by shear flow for $\dot{\gamma}\lesssim 4\ s^{-1}$ but is increased for all $\dot{\gamma}\gtrsim 4\ s^{-1}$. Our rheological measurements indicate that shear stress dominates for $\dot{\gamma}<4\ s^{-1}$ and that normal stresses dominate for $\dot{\gamma}>4\ s^{-1}$. Thus, the global enhancement in scattering for $\dot{\gamma}\gtrsim 4\ s^{-1}$ is coincident with normal stresses becoming dominant over shear stresses within the fluid.

In Fig. 4, we show the $\mathbf{q}$ dependence of the scattering at two different shear rates along the q_x and q_y axes. For $\dot{\gamma}=1.2\ s^{-1}$, there is no enhancement in the light scattering along the q_y axis [see Fig. 4(a), $\beta=90°$]. The same behavior is observed for all $\dot{\gamma}\lesssim 4\ s^{-1}$. By contrast, for $\dot{\gamma}=10\ s^{-1}$, the scattering intensity increases monotonically with decreasing q along the q_y axis [see Fig. 4(b)]. This increase at low q_y is observed only when $\dot{\gamma}\gtrsim 4\ s^{-1}$, or, once again, in the regime where the normal stresses become dominant over the shear stress. Along the q_x axis, there is a peak at finite q for the entire range of $\dot{\gamma}$ measured. As shown in Fig. 4, the peak height increases with increasing shear rate.

Our measurements immediately rule out several mechanisms which have been proposed to explain the shear-induced enhancement in light scattering. The alignment of the scattering maxima at $\beta\sim 40°$ for low shear is inconsistent with a recently proposed theory in which the chemical potential of a monomer is a function of the local stretch of the polymer.[8] The fact that we observe qualitatively different behavior at low shear rates, where the shear stress dominates, and at large shear rates, where the normal stress dominates, suggests that recent quasithermodynamic theories, which attribute the entire effect to normal stresses, are at best incomplete.[2] Moreover, these theories cannot account for the complexity of the structures which emerge under shear flow.

By contrast, many of our observations are qualitatively similar to predictions of a model recently proposed by Helfand and Fredrickson[7] (HF) and elaborated on by others.[9,11] The most notable similarity is that for low rates of shear, $\dot{\gamma}\tau_d<1$, $S(\mathbf{q})$ distorts such that fluctuations are enhanced along $\beta\simeq 45°$ and suppressed along $\beta\simeq 135°$ (see Figs. 2 and 3). Within HF, these low-shear-rate structures arise from a coupling between the concentration fluctuations and the velocity field via the concentration dependence of the viscosity. As the shear rate increases, the scattering pattern $S(q_x,q_y,\dot{\gamma})$ moves clockwise due to two effects. The first effect arises purely from convection and can be understood by considering the effect of convection on a sinusoidal concentration fluctuation born at a given wave vector, $[q_x(0),q_y(0)]$, at time $t=0$. The shear flow rotates the fluctuation in real space such that in q space it follows the trajectory $[q_x(t),q_y(t)]=[q_x(0),q_y(0)-\dot{\gamma}q_x(0)t]$. This is a model-independent feature of simple shear flow. Physically, this result means that the fluctuations which appear at a given $\mathbf{q}$ are not stationary in time but are con-

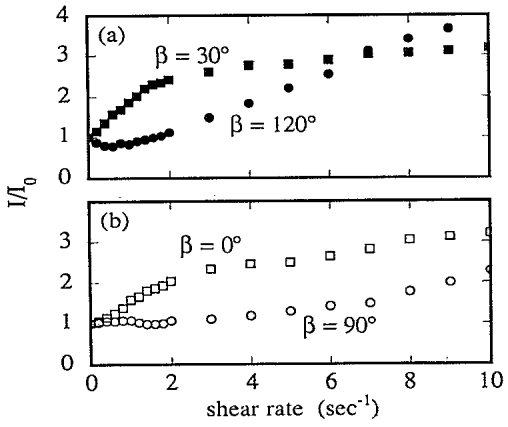

FIG. 3. Normalized scattering intensity vs shear rate ($\theta=90°$, $q=20.8\ \mu m^{-1}$). (a) $\beta=30°$ and $\beta=120°$, (b) $\beta=0°$ and $\beta=90°$.

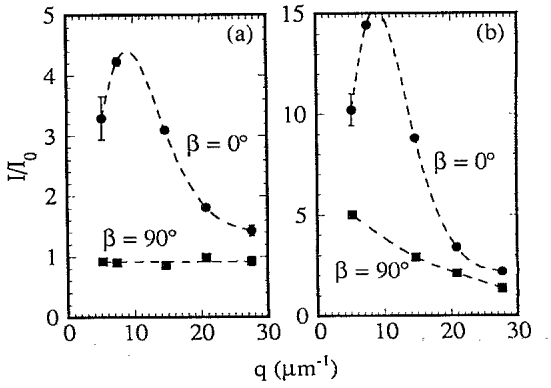

FIG. 4. Normalized scattering intensity vs q along the q_x and q_y axes for (a) $\dot{\gamma}=1.2\ s^{-1}$ and (b) $\dot{\gamma}=10\ s^{-1}$. Dashed curves serve as a guide to the eye.

tinuously being convected into and then out of that particular **q**. This is to be contrasted with the equilibrium situation in which fluctuations born at a given **q** remain at that same **q** until they dissipate some time later.

Within the HF model, the convection of fluctuations leads to a general rotation of $S(\mathbf{q})$ such that the regions of enhanced scattering produced by the concentration-dependent viscosity move toward, but not beyond, the q_x axis as the shear rate is increased. A second mechanism within HF that leads to a further rotation of $S(\mathbf{q})$ arises from the concentration-dependent *normal stresses* in the fluid and becomes significant only at high shear rates, $\dot{\gamma}\tau_d > 1$. Neglecting convection, this mechanism produces a ridge of maxima in $S(\mathbf{q})$ along the q_x axis where $\beta=0$. However, convection will rotate the maxima clockwise so that they move below the q_x axis and, within HF, asymptotically approach $\beta\sim -45°$ for very high rates of shear, $\dot{\gamma}\tau_d \gg 1$. This prediction is consistent with our measurements shown in Fig. 2. It is also interesting to point out that in binary liquid mixtures[3] and polymer mixtures,[6] where the strong coupling between local monomer concentration and flow is absent, there is no shear-induced enhancement in fluctuations, even though the latter exhibit very large viscosities and normal stresses. These observations and our results lend support to the basic HF mechanisms.

An important feature in our measurements of $S(\mathbf{q})$ is the peak that develops at low shear rates near $q_x \approx q_y \approx 10\ \mu\text{m}^{-1}$ and which moves towards $q_x \approx -q_y \approx 6\ \mu\text{m}^{-1}$ at high shear rates. This length scale is not accounted for within the HF theory. For small $\dot{\gamma}$, HF predict that $S(\mathbf{q},\dot{\gamma})\sim q^2$ along the direction of maximum growth, $\beta=45°$. However, this mechanism requires that the natural lifetime of fluctuations, $1/Dq^2$, be long compared to the time τ_d needed for elastic stresses to induce relative flow between the polymer and solvent.[7,16] Thus, the HF mechanism is suppressed for $q > q_m \equiv 1/(D\tau_d)^{1/2}$; this leads to a peak in $S(\mathbf{q},\dot{\gamma})$ at $q\sim 1/(D\tau_d)^{1/2}$. We measure $D=0.02\ \mu\text{m}^2/\text{s}$ from quasielastic light scattering and $\tau_d=0.57$ s from rheological measurements; this gives $q_m=9.4\ \mu\text{m}$, which is consistent with our data.

Finally, we would like to comment on the effect of shear flow on the phase stability of the solution. It is well known that when a system like a binary liquid mixture or polymer solution is quenched into the two-phase region, there is a spontaneous growth of domains. In a typical scattering experiment, a ring develops in the forward direction and then collapses as the domain size grows much larger than the scattering wavelength. In addition, hysteresis in the scattering intensity is observed upon a reverse quench into the single-phase regime. We have not been able to induce any of these effects using shear, even for $\dot{\gamma} \gtrsim 4\ \text{s}^{-1}$ where scattering is enhanced for all q. In particular, we have examined the transient relaxation at several scattering angles upon ceasing the shear flow and have observed no hysteresis on relaxing to the equilibrium state. Instead, after a fast elastic component due to recoverable strain, the transient measurements follow a slow, exponential decay with a time constant of ~ 2 s.

Another signature of an incipient phase transition is an increase in scattering at low q. In a sheared system, such an effect would be most unambiguous along the q_y axis ($\beta=90°$) where fluctuations are not convected by the shear flow. For $\dot{\gamma} \lesssim 4\ \text{s}^{-1}$, the data are qualitatively similar to those shown in Fig. 4(a), and show no enhancement in scattering anywhere along the q_y axis. Thus, we find no evidence that shear flow induces a phase transition for $\dot{\gamma} \lesssim 4\ \text{s}^{-1}$. By contrast, for $\dot{\gamma} \gtrsim 4\ \text{s}^{-1}$, there is a significant increase in the scattering at small q along the q_y axis, as illustrated in Fig. 4(b). This suggests that for high rates of strain, shear flow may move the phase boundary. However, we have never observed any macroscopic phase separation in the system. Thus, we have no clear evidence for a shear-induced phase transition.

We have benefited from discussions with S. Milner, A. Onuki, G. Fredrickson, D. Pearson, and W. Graessley. We also thank R. Gartner and D. Lohse for assisting with the rheology measurements.

[1]G. Ver Strate and W. Philippoff, Polymer Lett. **12**, 267 (1974).

[2]C. Rangel-Nafaile, A. B. Metzner, and K. F. Wissbrun, Macromolecules **17**, 1187 (1984).

[3]D. Beysens, M. Gbadamassi, and L. Boyer, Phys. Rev. Lett. **43**, 1253 (1979).

[4]A. Onuki and K. Kawasaki, Ann. Phys. (N.Y.) **121**, 456 (1979).

[5]A. I. Nakatani, Y. Takahashi, and C. C. Han, Polymer Commun. **30**, 43 (1989).

[6]T. Hashimoto, T. Takebe, and K. Fujioka, in *Dynamics and Patterns in Complex Fluids: New Aspects of Physics and Chemistry Interfaces,* edited by A. Onuki and K. Kawasaki (Springer, Berlin, 1990).

[7]E. Helfand and G. H. Fredrickson, Phys. Rev. Lett. **62**, 2468 (1989).

[8]A. Onuki, Phys. Rev. Lett. **62**, 2472 (1989).

[9]S. T. Milner, Phys. Rev. Lett. **66**, 1477 (1991).

[10]M. Doi, in Ref. 6.

[11]A. Onuki, J. Phys. Soc. Jpn. **59**, 3423 (1990).

[12]C. K. Chan, F. Perrot, and D. Beysens, Phys. Rev. Lett. **61**, 412 (1988).

[13]H. J. M. Hanley, J. C. Rainwater, N. A. Clark, and B. J. Ackerson, J. Chem. Phys. **79**, 4448 (1983).

[14]D. J. Evans, H. J. Hanley, and S. Hess, Phys. Today **37**, No. 1, 26 (1984).

[15]Temperature-dependent results will be published elsewhere.

[16]S. T. Milner (private communication).